Fluorescence Lifetime Imaging and FRET-Induced Intracellular Redistribution of Tat-Conjugated Quantum Dot Nanoparticles through Interaction with a Phthalocyanine Photosensitiser

*Elnaz Yaghini, Francesca Giuntini, Ian M. Eggleston, Klaus Suhling, Alexander M. Seifalian, and Alexander J. MacRobert**

The interaction of Tat-conjugated PEGylated CdSe/ZnS quantum dots (QD) with the amphiphilic disulfonated aluminium phthalocyanine photosensitiser is investigated in aqueous solution and in a human breast cancer cell line. In aqueous solution, the QDs and phthalocyanine form stable nanocomposites. Using steady-state and time-resolved fluorescence measurements combined with singlet oxygen detection, efficient Förster resonance energy transfer (FRET) is observed with the QDs acting as donors, and the phthalocyanine photosensitiser, which mediates production of singlet oxygen, as acceptors. In cells, the Tat-conjugated QDs localise in lysosomes and the QD fluorescence lifetimes are close to values observed in aqueous solution. Strong FRET-induced quenching of the QD lifetime is observed in cells incubated with the nanocomposites using fluorescence lifetime imaging microscopy (FLIM). Using excitation of the QDs at wavelengths where phthalocyanine absorption is negligible, FRET-induced release of QDs from endo/lysosomes is confirmed using confocal imaging and FLIM, which is attributed to photooxidative damage to the endo/lysosomal membranes mediated by the phthalocyanine acceptor.

1. Introduction

Quantum dot (QD) nanoparticles exhibit significant advantages for cellular labelling and in vivo imaging compared to standard organic dyes owing to their intense photoluminescence (PL) and resistance to photobleaching.[1–4] However, wider application of QDs to intracellular and molecular imaging has been hindered by their limited ability to penetrate cell membranes, and much effort has therefore been directed towards improving uptake of QDs into cells. In particular, the use of cell-penetrating peptide sequences, such as oligoarginine or Tat has been shown to be effective for mediating efficient cellular uptake.[5] The Tat (48–57) sequence derived from human immunodeficiency virus (HIV)-1 is one

Dr. E. Yaghini, Prof. A. J. MacRobert
National Medical Laser Centre
Division of Surgery & Interventional Science and UCL Institute for Biomedical Engineering
University College London, London, UK
E-mail: a.macrobert@ucl.ac.uk
Dr F. Giuntini, Dr. I. M. Eggleston
Wolfson Laboratory of Medicinal Chemistry
Department of Pharmacy and Pharmacology
University of Bath, Bath, UK

DOI: 10.1002/smll.201301459

Dr. K. Suhling
Department of Physics
King's College London, London, UK
Prof. A. M. Seifalian
Centre for Nanotechnology and Regenerative Medicine
Division of Surgery and Interventional Science
University College London, London, UK

NANO MICRO small

of the most commonly used cell-penetrating peptides for transporting various cargos into the cells.[6–11] Tat-conjugated QDs are known to be taken up via endocytosis and become entrapped within endo/lysosomal vesicles. In a high resolution confocal imaging study, Ruan and colleagues demonstrated that Tat-conjugated QDs are tethered to the inner surface of these vesicles as a result of electrostatic interaction between the cationic QD surface and the negatively charged vesicle lipid membrane.[5]

A number of strategies to induce the release of endo/lysosmally confined agents including nanoparticle drug carriers have been designed to overcome this limitation, including the use of photosensitisers for photochemically-mediated rupture of the endo/lysosomal membranes. This technique is known as Photochemical Internalisation (PCI) and is derived from photodynamic therapy (PDT), which uses photosensitive compounds to trigger light-targeted cell killing via the production of reactive oxygen species (ROS), in particular singlet oxygen ($^1O_2$). In the PCI approach, a sub-lethal light dose is applied to a photosensitiser (PS) that localises in endo/lysosomal membranes, which is sufficient to induce rupture of the membranes of these intracellular organelles, but less than that required to kill the whole cell. The photo-induced rupture of the endo/lysosomal membrane via singlet oxygen mediated oxidation of membrane constituents (e.g, unsaturated lipids, cholesterol) then enables release of entrapped agents from the central aqueous compartment of the endo/lysosomes. The delivery of a variety of different macromolecular agents including; cytotoxic chemotherapeutics, antibodies and genes have been potentiated by PCI.[12–17] The photosensitiser may also be incorporated in a nanovehicle bearing the bioactive agent, and PCI has been shown to improve intracellular delivery and efficacy of cytotoxic agents.[18]

To date PCI has employed direct excitation of the photosensitiser, in most cases a porphyrin or phthalocyanine derivative, to induce the endo/lysosomal release of the entrapped bioactive agent. Alternatively, excitation of the photosensitiser via Förster Resonance Energy Transfer (FRET) using an entrapped nanovehicle with suitable photophysical properties should be feasible. QDs have been widely used as energy donors in a variety of FRET-based biological studies, since they offer several advantages making them well suited to serve as energy donors.[19,20] Firstly, the narrow emission and broad absorption spectra of QDs, enables the effective separation of the donor and acceptor fluorescence, and the selection of a wide range of excitation wavelengths to reduce direct excitation of the acceptor. Secondly, the large size of the QDs allows design of a simple configuration where multiple acceptor molecules can interact with a single donor molecule which substantially enhances the overall efficiency of FRET between donor/acceptor pairs.[19–21]

Since QDs can be very efficient FRET donors, we have evaluated the combination of a phthalocyanine photosensitiser with QDs to induce endo/lysosomal release of the QDs via the FRET mechanism. The key requirement for this mechanism to operate is close proximity of the QD and the PS, and several groups have reported the occurrence of FRET in QD-PS complexes or hybrids to generate ROS in aqueous solution as reviewed by Yaghini et al.[22] The key ROS intermediate in this approach is $^1O_2$ which can be produced with significant quantum yields. Burda and co-workers reported FRET in CdSe QDs conjugated to a silicon phthalocyanine (Pc4) using excitation at 488 nm where the phthalocyanine absorption is negligible.[23] Although a 77% FRET efficiency was reported, the conjugate was not soluble in water and therefore not directly applicable in biological systems. Tsay et al., utilised peptide coated QD-PS hybrids to generate $^1O_2$ via FRET from QD to PS.[24] The photosensitisers, Rose Bengal and chlorin e6, were coupled to peptides, which in turn were conjugated to CdSe/CdS/ ZnS QDs. The quantum yield of the formation of $^1O_2$ either via direct excitation of PS or indirectly through the FRET mechanism was observed ranging from 0.09–0.31 depending on the QD-PS combination and excitation wavelength. Recently Lai and co-workers have also demonstrated bioluminescence resonance energy transfer between Renilla luciferase-immobilized quantum dots, which exhibited peak emission at 655 nm after addition of coelenterazine, and a chlorin photosensitiser.[25]

Most of the studies reported on QD-PS conjugates have been confined to organic solvents or aqueous solutions. In this study we investigated the efficiency of Tat-conjugated QD-PS nanocomposites to perform as donor/acceptor pairs in both aqueous solution and living cells. For this purpose an amphiphilic photosensitiser was selected, disulfonated aluminium phthalocyanine ($AlPcS_{2a}$), which can bind to the QDs and has been used previously in photochemical internalisation studies owing to its favourable phospholipid membrane localization.[16,26,27] This phthalocyanine has amphiphilic properties since the two sulfonate groups are substituted on adjacent benzo rings (as shown in Figure S1a Supporting information) so that the hydrophobic unsubstituted side of the molecule can penetrate into the lipid phase. The photophysical properties of $AlPcS_{2a}$ have been reviewed by Phillips et al.[28] Using a combination of steady-state confocal and fluorescence lifetime imaging microscopy (FLIM) we were able to demonstrate for the first time intracellular photo-induced release of Tat-QDs from endo/lysosomal vesicles via the FRET mechanism.

2. Results and Discussion

2.1. Synthesis of QD-$AlPcS_{2a}$ Nanocomposites

Tat-conjugated CdSe/ZnS QDs with an emission peak at 620 nm were prepared by conjugating a peptide containing the HIV-1 Tat (48–57) sequence with an amine functionalised polyethylene glycol (PEG) coating on the QDs.[14] Aluminium disulfonated phthalocyanine ($AlPcS_{2a}$) with two adjacent sulfonated groups was selected as the photosensitiser and acceptor for the FRET studies owing to the good spectral overlap with the QD, and its water solubility. At neutral pH, the primary amino groups of the QD and the amino and guanidino groups of the respective lysine and arginine side chains of the Tat peptide are protonated based on their high pKa > 10 values: Ruan at el. reached the

same conclusion in their study on Tat-QDs.[5] It was hypothesised that the positively charged Tat-conjugated QDs would therefore bind electrostatically with the negatively charged $AlPcS_{2a}$ photosensitiser. Dilute aqueous QD solutions (100 nM) were mixed with increasing phthalocyanine concentrations from 100–800 nM to produce nanocomposites or complexes with different molar ratios of phthalocyanine to QD.

2.2. FRET between QDs and $AlPcS_{2a}$

The formation of QD-$AlPcS_{2a}$ nanocomposites and occurrence of FRET was examined by steady-state and time-resolved fluorescence measurements using excitation at 405 nm at which the phthalocyanine exhibits minimal absorption, as confirmed in control experiments with only the phthalocyanine present. Using steady-state fluorescence measurements, a significant decrease in QD emission with a parallel enhancement in the phthalocyanine fluorescence was observed upon mixing of the two components, indicating non-radiative energy transfer from photoexcited QD donor to ground state photosensitiser acceptor (Supporting information, Figure S1b). The good overlap between the QD emission and absorption spectra of the phthalocyanine favours non-radiative energy transfer within QD-phthalocyanine donor/acceptor pair, as shown in the Supporting information, Figure S2. The Förster distance (R_0) was derived as 5.9 nm. The calculated values correspond with other FRET studies on quantum dot-dye donor/acceptor pairs.[29]

It has been previously reported that the FRET efficiency increases when the number of acceptors per QD increases.[30] We also found that the decrease in QD emission intensity was dependent on the phthalocyanine/QD molar ratio, since with increasing stoichiometric molar ratios, the QD emission progressively decreased. Further confirmation for the occurrence of FRET was provided by QD donor lifetime measurements using time-correlated single photon counting (TCSPC). Biexponential decay analysis of the QD time-resolved photoluminescence intensity (I_t) was carried out using the equation, $I_t = A_1\exp(-t/\tau_1) + A_2\exp -t/\tau_2)$, where A and τ are the fractional amplitude and lifetime.[31,32] Although the donor acceptor distance may vary, thus yielding varying FRET efficiencies and complex decay kinetics, we use a biexponential decay model, as others have done.[33] Rather than analyzing single decay traces, our emphasis is on FRET imaging using FLIM and in view of the FLIM photon statistics, the use of more complex decay models in a single pixel is not really statistically justified.[34]

Table 1. Photoluminescence (PL) emission lifetimes/ns (τ) and fractional amplitudes (A) of Tat-conjugated CdSe/ZnS QDs in aqueous solution (100 nM) and MCF-7 cells incubated with 50 nM of QDs for 24 h. Biexponential fitting was employed with the shorter lifetime designated as τ_1 for ease of comparison.

QD emission lifetime τ/ns and fractional amplitudes (A)	$\tau_1/(A_1)$	$\tau_2/(A_2)$
Aqueous solution	4.5 (0.4)	21 (0.6)
MCF-7 cells	5.5 (0.6)	18 (0.4)

Biexponential fitting to QD decays in aqueous solution gave satisfactory fits showing a short lifetime component of $\tau_1 = 4.5$ ns and a long lifetime component of $\tau_2 = 21$ ns and comparable fractional amplitudes (**Table 1**). A substantial shortening of the QD donor decay was observed in the presence of the phthalocyanine acceptor (**Figure 1**A). At highest molar stoichiometric ratio of $AlPcS_{2a}$/QD (N = 8), biexponential fitting yielded a major short lifetime component of $\tau_1 = 2.1$ ns ($A_1 = 0.85$), and a minor long lifetime component of $\tau_2 = 10.4$ ns ($A_1 = 0.15$) respectively. The fractional amplitude weighted mean lifetime of QDs in the absence of phthalocyanine was found to be $\tau_D = 14.4$ ns which was considerably reduced when the phthalocyanine acceptor (molar ratio of 8) was present in the solution, $\tau_{DA} = 3.4$ ns. The FRET efficiency (E) was calculated as 76% for this molar ratio, using the equation, $E = 1 - (\tau_{DA}/\tau_D)$.

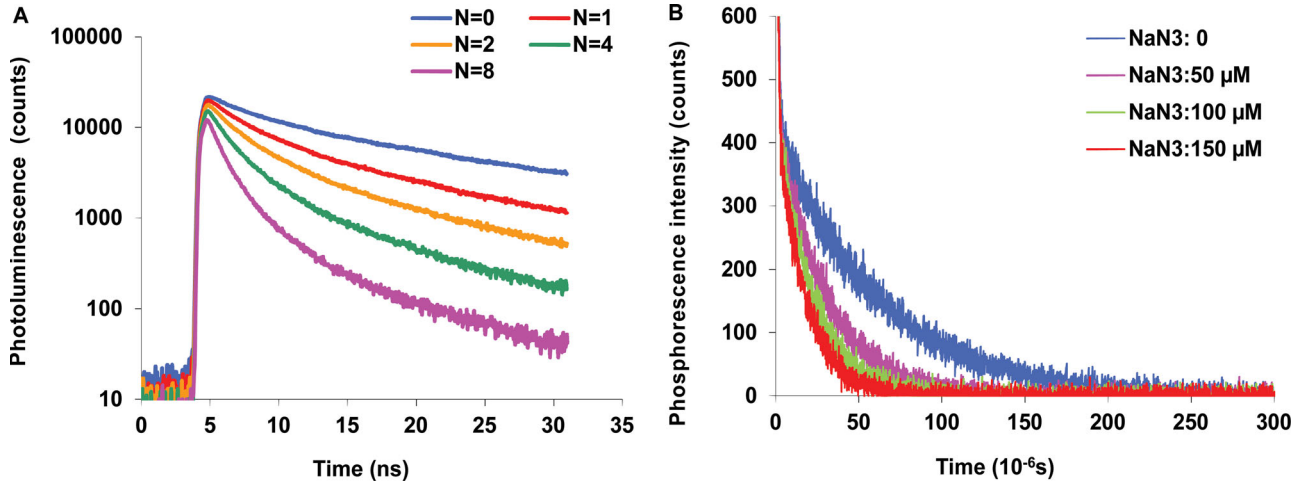

Figure 1. (A) Logarithmic plots of time-resolved QD PL decays of Tat-QD-$AlPcS_{2a}$ complexes, measured using time-correlated single photon counting with excitation at 405 nm. The molar ratio of $AlPcS_{2a}$/QD varies from N = 0 to 8 with a QD concentration of 100 nM; (B) Time-resolved singlet oxygen phosphorescence decays for air-saturated deuterated solutions of Tat-QD-$AlPcS_{2a}$ complexes (molar ratio of $AlPcS_{2a}$/QD of 8, QDs at 100 nM) at increasing NaN_3 concentrations (0–150 µM).

NANO MICRO small

Binding of the phthalocyanine to the PEGylated QD would result in a change in microenvironment and a small 3 nm blue shift in the phthalocyanine absorption Q-band peak was observed (data not shown). A similar blue shift is observed when $AlPcS_{2a}$ was dissolved in MeOH vs. aqueous solution.[35,36] Moreover, the fluorescence lifetime of the $AlPcS_{2a}$ in the presence of the QDs was longer (6.9 ns compared to 5.0 ns in aqueous solution) than that of without QDs, again consistent with a change in the microenvironment of the phthalocyanine due to incorporation in the PEGylated layer. There were no obvious changes in the absorption spectrum of the QDs after combination with phthalocyanine. Similar behaviour using steady-state spectroscopy has been reported previously by Shi et al., following mixing of tetra (4-sulfonatophenyl) porphyrin (TPPS) with QDs which was attributed to the attachment of the porphyrin to the nanocrystal surface.[37] The tetrasulfonated aluminium phthalocyanine has been reported to form complexes with thiol-capped CdTe QDs.[38] However, one significant difference in the method of complexation used here is that the QD is encapsulated within a PEGylated layer so that the phthalocyanine must be able to penetrate this layer in order to approach the QD surface for FRET to take place.

$AlPcS_{2a}$ is a relatively lipophilic molecule and is known to partition to liposomal membranes and organelle membranes in cells.[17,39] This is probably as a result of the adjacent location of the charged sulfonate groups on one side of the macrocycle leaving the unsubstituted part of macrocycle relatively hydrophobic which would promote localisation near the surface of the lipid bilayer. It is therefore reasonable to propose that this phthalocyanine can partition to the PEGylated layer surrounding the QD to form a complex with the QD. Complexation of a silicon phthalocyanine (Pc4) photosensitiser with a PEGylated gold nanoparticle has recently been reported by Cheng et al.[40,41] The side chains attached to the central silicon which are terminated with amino groups may also permit direct binding with the gold surface. These nanocomposites were then used for delivery of the phthalocyanine to tumor cells for photodynamic therapy. Gold nanorod-phthalocyanine complexes have also been investigated for PDT and photothermal therapy and the chlorin e6 photosensitiser, which has similar amphiphilic properties to $AlPcS_{2a}$, has been shown to form stable complexes with PEGylated upconversion nanoparticles.[42–44]

The steady state and time resolved fluorescence measurements both demonstrate that PEGylated CdSe/ZnS QD-$AlPcS_{2a}$ complexes can perform as an efficient donor/acceptor pair in a FRET-based system. The fact that a molar excess of phthalocyanine is required over the QD implies that binding of several phthalocyanine molecules is necessary for efficient FRET, since complexation with multiple acceptors leads to enhanced FRET efficiency.[31]

The diameter of the QD core is <10 nm but with the PEG coating the resulting hydrodynamic diameter is ~25 nm (according to specifications provided by the manufacturer) therefore the phthalocyanine must have penetrated within the PEG coating upon complexation to achieve efficient FRET.

We also investigated the production of $^1O_2$ from the QD-phthalocyanine complexes. FRET results in formation of the phthalocyanine acceptor excited singlet state which then either fluoresces or undergoes intersystem crossing to produce the triplet state. The triplet state then interacts with molecular oxygen within the PEGylated layer to generate $^1O_2$ which can diffuse out of the layer into the solution. The efficiency of the QD complexes to produce $^1O_2$ via FRET was examined using time-resolved detection of $^1O_2$ phosphorescence at 1270 nm (Figure 1B). Monoexponential decays were observed using deuterated solutions (to reduce the rate of physical quenching) with a decay lifetime consistent with the known lifetime of singlet oxygen in D_2O (68 μs) showing that the singlet oxygen generated diffuses out of the PEGylated layer.[28] Addition of sodium azide (NaN_3) a well-known $^1O_2$ scavenger resulted in strong suppression of the $^1O_2$ production. In control experiments, using only QDs or phthalocyanine, no $^1O_2$ was generated, confirming that the detected $^1O_2$ phosphorescence from QD complexes was due to the FRET mechanism.

Using Rose Bengal as reference compound, the $^1O_2$ quantum yield for the QD complexes was calculated using a time-gated integration analysis method since the standard zero intercept analysis was ruled out by the relatively high residual QD emission even at the NIR detection band.[45] A $^1O_2$ quantum yield of ~0.1 was obtained for the Tat-QD-$AlPcS_{2a}$ complexes at a molar ratio of 8. This yield is slightly lower than the yield of free $AlPcS_{2a}$ in deuterated aqueous solution for which a value of 0.17 has been measured.[46] The fact that a lower value is found is not surprising since the complexation is a saturable process so the values obtained here are underestimates. The azide quenching rate constant (4.4×10^8 M^{-1} s^{-1}) measured for the QD complexes is in good agreement with the value for $^1O_2$ produced in aqueous solution from conventional photosensitisers.[47] Singlet oxygen generation by CdSe QDs has been reported by Samia et al., in toluene, but was not detected by Shi et al., for CdTe QDs in water and we could not detect any $^1O_2$ generation from either the un-conjugated or Tat-peptide conjugated QDs alone.[37,48]

2.3. Intracellular Studies of FRET and Photo-induced QD Redistribution

We have shown that the Tat-conjugated CdSe/ZnS QDs and $AlPcS_{2a}$ photosensitiser can act as an efficient donor/acceptor pair for FRET in aqueous solution. We then investigated the occurrence of FRET in living cells, using laser scanning confocal microscopy (LSCM) and fluorescence lifetime imaging microscopy (FLIM).[49–51]

MCF-7 human breast carcinoma cells were incubated with QDs alone or with QD complexes generated using a phthalocyanine/QD molar ratio of 10 and a QD concentration of 50 nM in serum-free medium. Cells were incubated for 24 h as we had previously established maximum uptake of the Tat-conjugated QDs occurred at 24 h. LSCM images revealed that Tat-QDs (without the phthalocyanine) were predominantly localised in extranuclear vesicles and co-localised with LysoTracker Green, confirming lysosomal sequestration of the Tat-QD conjugates in agreement with

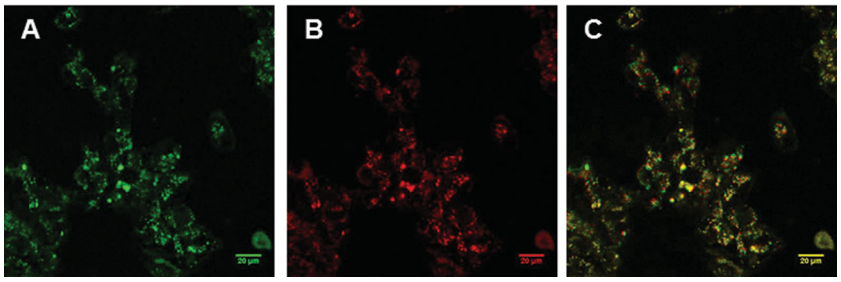

Figure 2. Fluorescence laser scanning confocal microscopy of MCF-7 cells using 488 nm excitation. Cells were incubated with Tat-CdSe/ZnS-AlPcS$_{2a}$ complexes (AlPcS$_{2a}$/QD molar ratio of 10) for 24 h (QDs: 50 nM, AlPcS$_{2a}$: 500 nM). QD emission (A) was detected in the donor channel, 590–640 nm. AlPcS$_{2a}$ fluorescence (B) detected in the acceptor channel, 670–700 nm. Yellow colour (C) represents the merged image of donor and acceptor fluorescence. Scale bar is 20 μm.

previous studies using Tat-conjugated QDs (Figure S3 Supporting Information).[5] The cellular uptake was also found to be inhibited at low temperature, demonstrating that the uptake of Tat-QD conjugates was energy-dependent, which is consistent with an endocytic uptake mechanism. In control experiments when cells were incubated with QDs but without conjugation to the Tat peptide, intracellular QD PL was negligible, confirming that the Tat peptide is an effective vehicle for delivery of QDs into the cells.[5]

The occurrence of FRET between Tat-CdSe/ZnS and AlPcS$_{2a}$ in the cells was then evaluated using LSCM. Cells were incubated with Tat-CdSe/ZnS-AlPcS$_{2a}$ QD complexes for 24 h and excitation was carried out at 488 nm in order to avoid direct excitation of AlPcS$_{2a}$. Fluorescence images of QDs and the phthalocyanine were detected in the donor and acceptor channels respectively, as shown in **Figure 2**. The yellow colour (Figure 2C) shows the merged image of the donor and acceptor channel, demonstrating a good co-localisation of QDs with the phthalocyanine, within the spatial resolution limit. A punctate pattern was observed corresponding to lysosomal localisation. Lysosomal localisation has previously been observed for low density lipoprotein (LDL) – AlPcS$_{2a}$ complexes in fibroblasts.[52]

In control experiments, excitation of the cells containing only AlPcS$_{2a}$ at 488 nm resulted in a negligible signal in the acceptor channel, precluding direct excitation of the photosensitiser at this wavelength. Likewise for cells containing only QDs, no PL was observed in the acceptor channel. These results indicate that FRET between the Tat-QD and the phthalocyanine can occur in cells. Further confirmation was provided using FLIM as described later.

Since we know that the Tat-conjugated QDs are confined within the aqueous compartment of endo/lysosomes in agreement with a previous study, then drawing upon the photochemical internalisation concept, we investigated whether reactive oxygen species (ROS) generation using a photosensitiser can be used to release QDs either through direct excitation of the photosensitiser or via an indirect FRET mechanism.[5]

Using the same incubation conditions as for Figure 2, PL images of QDs were acquired at regular intervals following irradiation at 488 nm. Periodically fluorescence images were acquired with 633 nm excitation which directly excites the phthalocyanine but not the QD, so that the redistribution of the phthalocyanine could be separately monitored. Care was taken to use short exposures with 633 nm that did not perturb the intracellular distributions. As shown in **Figures 3**A and B, initially a clear punctuate pattern of distribution was observed for QDs and phthalocyanine. Upon extended on-stage irradiation at 488 nm, significant changes in the distribution pattern were observed for both QDs and phthalocyanine (Figure 3C and D). The intracellular distribution of QD

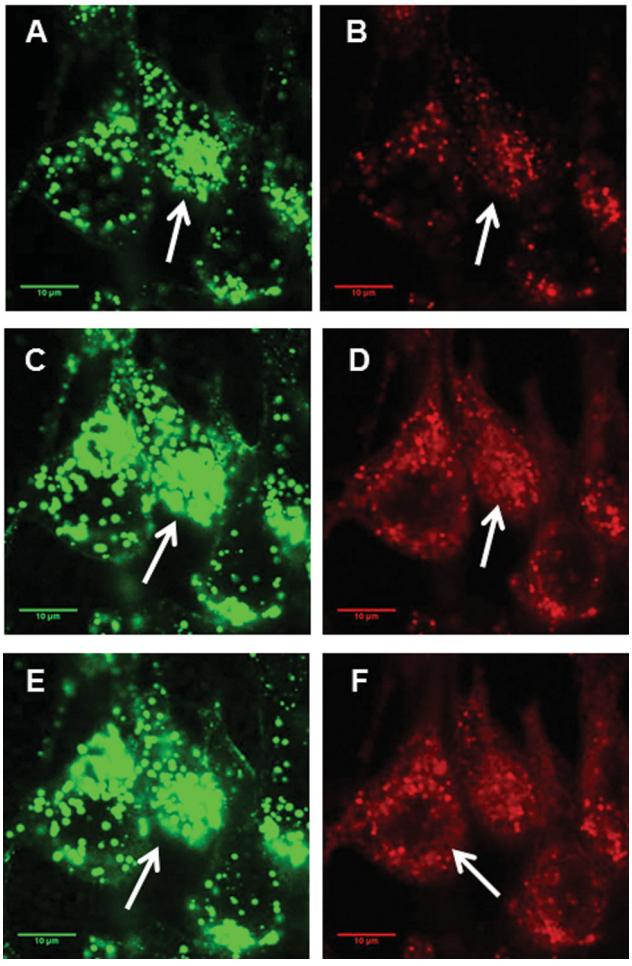

Figure 3. Effect of irradiation using 488 nm laser on intracellular distributions of Tat-conjugated CdSe/ZnS QDs and AlPcS$_{2a}$ in MCF-7 cells following incubation with Tat-CdSe/ZnS-AlPcS$_{2a}$ complexes (AlPcS$_{2a}$/QD molar ratio of 10) for 24 h (QDs: 50 nM, AlPcS$_{2a}$: 500 nM). The 488 nm laser of the confocal microscope was used as the irradiation light source. A and B show initial distributions of QDs (A) and phthalocyanine (B); C and D after 1 min of 488 nm irradiation; E and F after 2 min on-stage irradiation. PL of QDs (green images) detected in the range 590–640 nm using 488 nm excitation. AlPcS$_{2a}$ fluorescence (red images) detected in the range 670–700 nm using 633 nm excitation. The white arrows show redistribution of QDs and AlPcS$_{2a}$. Scale bar is 10 μm.

NANO MICRO small

PL and phthalocyanine fluorescence changed from the initial punctate pattern to more diffuse staining after irradiation (see white arrows). After 2 min, a more diffuse spread of QDs and phthalocyanine was observed throughout the cytosol (Figure 3E and F), with less co-localisation. In control studies using cells incubated with the QDs only, no redistribution was evident for the same irradiation parameters (data not shown). These results demonstrate that FRET from the QD to the phthalocyanine photosensitiser to generate $^1O_2$ was capable of inducing intracellular redistribution of both the QD and the photosensitiser. Redistribution can occur following singlet oxygen oxidation of membrane components to induce rupture of the endo/lysosomes which then enables release of the inner aqueous compartment contents including the endocytosed QDs into the cytosol. The proximity of Tat-conjugated QDs to the inner lysosomal membrane due to electrostatic interaction favours singlet oxygen mediated photooxidative damage to the lysosomal membranes.[5]

We then investigated whether extended irradiation at 633 nm which directly excites the phthalocyanine (without indirect excitation via FRET since the QD does not absorb at 633 nm) could also induce intracellular fluorescence redistribution. For this purpose we used a higher phthalocyanine concentration at 1 μM in order to amplify the photo-induced response using the 633 nm excitation wavelength. The initial punctate localisation of the QD and phthalocyanine were very similar (**Figure 4**A and B). However following irradiation, the distributions of both QD and phthalocyanine were more noticeably diffuse, showing that the QDs and phthalocyanine had been dispersed from their initial pre-irradiation sites (Figure 4C and D). The QD emission was detected separately using 488 nm excitation but the light dose was insufficient to result in FRET-induced redistribution. The photo-induced redistribution of $AlPcS_{2a}$ observed here corresponds well with previous PCI studies in other cell lines.[13,17]

In summary, for both sets of experiments using either 488 or 633 nm irradiation, photoinduced redistribution of the QDs and the phthalocyanine from an initially punctate localisation to a more diffuse distribution was observed. In the case of 488 nm excitation, which excludes direct phthalocyanine excitation, we propose that this is due to FRET from the QD donor to the phthalocyanine acceptor leading to singlet oxygen generation. In control experiments when cells were incubated with QDs only, excitation at 488 nm under the same conditions did not lead to any detectable

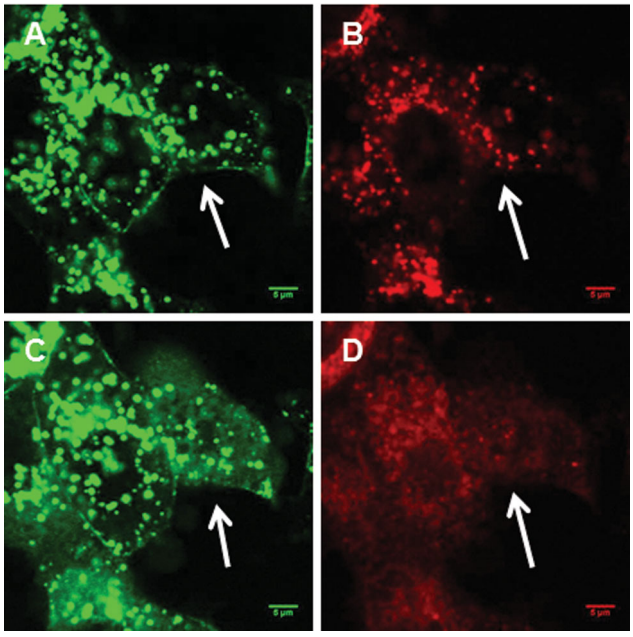

Figure 4. Effect of light irradiation using 633 nm to excite the phthalocyanine directly on intracellular fluorescence distributions of Tat-conjugated CdSe/ZnS QDs and $AlPcS_{2a}$ in MCF-7 cells following incubation with Tat-CdSe/Zn (50 nM) and $AlPcS_{2a}$ (1 μM) for 24 h. A and B show initial images of QDs and $AlPcS_{2a}$; C: QD distribution 4 min after 30 s irradiation, and D: $AlPcS_{2a}$ distribution 4 min after 30 s irradiation. The white arrows show redistribution of QDs and $AlPcS_{2a}$. PL of QDs (green images),detected in the range 590–640 nm using 488 nm excitation. $AlPcS_{2a}$ fluorescence (red images) was detected in the 670–700 nm range using 633 nm excitation. Scale bar is 5 μm.

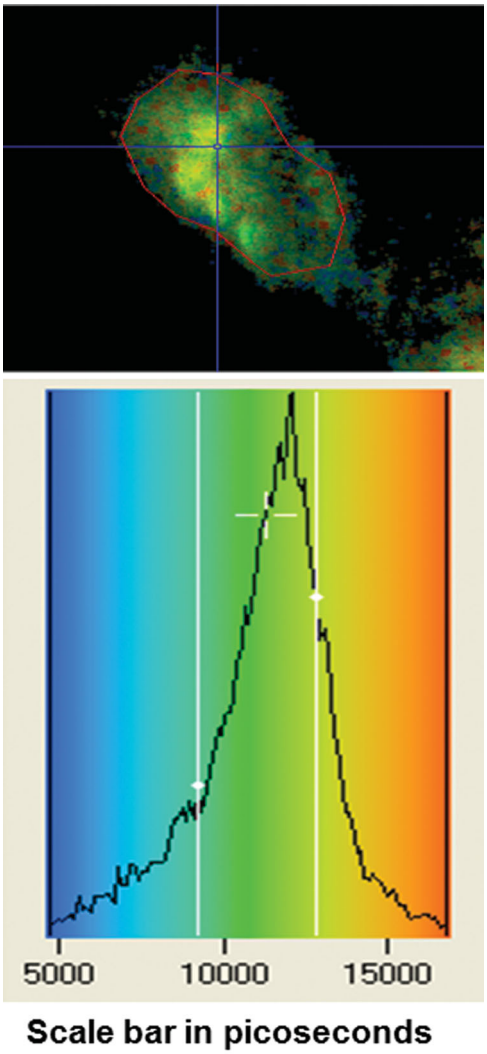

Figure 5. FLIM image of a whole cell and lifetime histogram of Tat-conjugated CdSe/ZnS QDs in the absence of $AlPcS_{2a}$.The red line delineates the area in the image used to analyse the mean lifetimes. The scale gives the lifetimes in ps, ie 10000 corresponds to 10 ns. Blue corresponds to a short lifetime, and red to a long lifetime. MCF-7 cells were incubated with QDs (50 nM) for 24 h.

change in the QDs distribution. This provided strong evidence that the observed lysosomal disruption and redistribution of QDs upon illumination was indeed due to the FRET-induced formation of singlet oxygen which can induce endo/lysosomal membrane damage. Further confirmation for this mechanism was obtained from FLIM studies as described below. These photo-induced changes are consistent with the mechanism of photochemical internalisation whereby moieties confined in endo/lysosomes can be released into the cytosol through photoinduced rupture of the vesicle membranes.[14,17,39] The PCI process by itself is not significantly cytotoxic (typically <30%) as we and other have shown but the photoinduced release of cytotoxic agents confined within the endo/lysosomes can lead to significant enhancement of cytotoxicity by two orders of magnitude.[14,17]

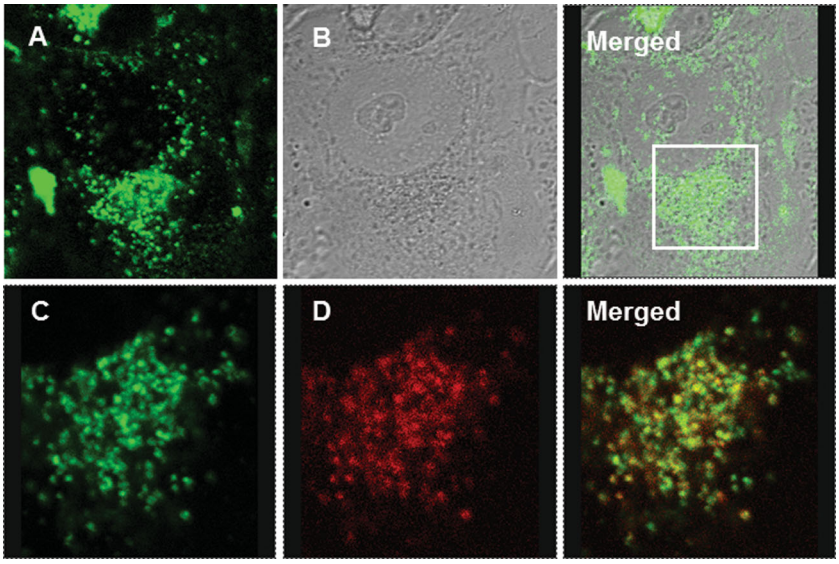

Figure 6. Confocal images of MCF-7 cells incubated with Tat-conjugated CdSe/ZnS-AlPcS$_{2a}$ complexes (AlPcS$_{2a}$/QD molar ratio of 10, QD: 50 nM) for 24 h using 470 nm excitation (A) and phase contrast images (B) of whole cell, with merged fluorescence-phase contrast images on right-hand side. White inset in the merged image highlights the subcellular region shown in subsequent C-D images. Initial images of QD PL (C), AlPcS$_{2a}$ fluorescence (D), and merged image on right side, with yellow colour showing good overlap between QDs and AlPcS$_{2a}$.

2.4. FLIM Studies of QDs in Cells

To further investigate the occurrence of the FRET in living cells, emission lifetimes of Tat-conjugated CdSe/ZnS QDs in the presence and absence of AlPcS$_{2a}$ were measured using the fluorescence lifetime imaging technique (FLIM) incorporating time-correlated single photon counting (TCSPC).[49] Unlike fluorescence intensity, the fluorescence lifetime is not dependent on the donor concentration, illumination intensity, moderate photobleaching or light path length, which are parameters that are difficult to control in a cellular system. In the FRET-FLIM-based approach, the detection of FRET is provided by monitoring the change in donor lifetime in the presence and absence of the acceptor.[53–58]

MCF-7 cells were incubated with either Tat-conjugated CdSe/ZnS QDs or Tat-conjugated CdSe/ZnS-AlPcS$_{2a}$ complexes for 24 h (QDs: 50 nM, AlPcS$_{2a}$: 500 nM) and cell images were acquired, using another LSCM equipped with FLIM capability. The QD complexes were prepared in the same way as for the steady-state studies, with the same incubation conditions. Excitation for acquiring steady-state and FLIM was carried out using a picosecond laser diode at 470 nm, for which phthalocyanine excitation is negligible, and images of QD PL and the phthalocyanine fluorescence were recorded. **Figure 5** shows a FLIM map across a whole cell and the corresponding histogram of the average fluorescence lifetime distribution of the QDs alone on a picosecond timescale. Because FLIM analysis uses far fewer photons the quality of the images is relatively poor compared to the steady-state images. Histogram analysis of the average lifetime distribution shows a maximum near 12 ns. Lifetimes were measured by analysing the integrated photon count in the cell image, since with this method a much higher number of photon counts can be analysed giving a more accurate determination of the lifetime. A more detailed analysis can be made by selecting points within the lifetime image using a cursor, as shown in Figure 5. Data were taken from 5 points with high photon counts and fitted biexponentially. An example of a fitted fluorescence decay is shown in the Supporting Information (Figure S4A). The short and long lifetime components of QDs were averaged to be $\tau_1 = 5 \pm 0.5$ ns and $\tau_2 = 18 \pm 2$ ns respectively. These values are close to the lifetimes of QDs measured in cell free aqueous solutions (Figure 1), shown in Table 1. As far as we are aware this is the first study to present such a comparison.

We then analysed steady-state and FLIM images acquired using incubation with the QD-phthalocyanine complexes. The merged emission-phase contrast image of cells showed that QDs exhibited a punctuate distribution throughout the cytosol (**Figure 6**A and B) in good agreement with the images shown in Figure 2A. For FLIM measurements, a subcellular area was selected (white inset) showing the punctate QD photoluminescence. With excitation at 470 nm a bright fluorescence signal was also detected in the acceptor channel (670–700 nm), implying indirect excitation of the phthalocyanine via FRET, as shown in Figure 6D. The punctuate fluorescence pattern is clearly evident in both the donor (Figure 6C) and acceptor (Figure 6D) channels with good co-localisation evident in the merged image, which is in good agreement with the images shown in Figure 2.

The FLIM image and lifetime histogram analysis of the same subcellular region is shown in **Figure 7**. The fluorescence lifetime of QDs was significantly shorter and the lifetime histogram of QDs showed a peak lifetime near 0.8 ns, in contrast to the broad distribution observed for the lifetime of QDs alone, with a peak value of 12 ns, shown in Figure 5. Biexponential fitting of the data using the cursor analysis gave a major short lifetime component of

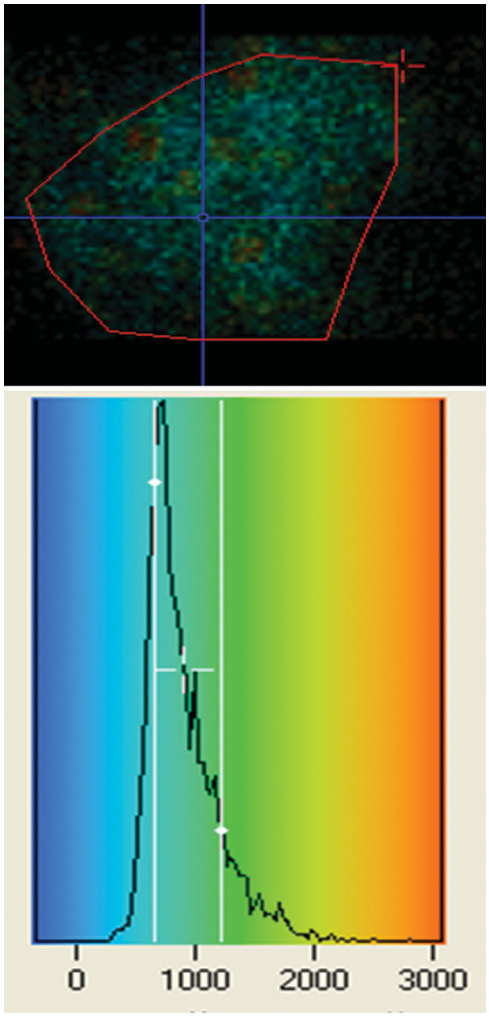

Figure 7. FLIM image of cells and lifetime histogram of Tat-conjugated CdSe/ZnS QDs following incubation with QD-$AlPcS_{2a}$ complexes over the same field as shown in Figure 6C The red line delineates the area in the image used to analyse the lifetimes. The scale gives the mean lifetimes in ps, ie 1000 corresponds to 1 ns. Blue corresponds to a short lifetime, and red to a long lifetime.

$\tau_1 = 0.8 \pm 0.2$ ns and, a long lifetime component of $\tau_2 = 6.6 \pm 0.2$ ns with much lower amplitude (**Table 2**). An example of a fitted fluorescence decay is shown in the Supporting Information (Figure S4B). The amplitude weighted mean lifetime is 1.2 ns, compared to 10.7 ns in the absence of the phthalocyanine.

Table 2. Photoluminescence (PL) emission lifetimes (τ) and fractional amplitudes (A) of Tat-conjugated CdSe/ZnS QDs in the presence and absence of $AlPcS_{2a}$ in aqueous solution (molar ratio of $AlPcS_{2a}$/QD, N = 8), and MCF-7 cells incubated with QD-$AlPcS_{2a}$ complexes for 24 h.

QD emission lifetime τ/ns and fractional amplitudes (A)	$\tau_1/(A_1)$	$\tau_2/(A_2)$
Aqueous solution (only QDs)	4.5 (0.4)	21 (0.6)
Aqueous solution (QDs-$AlPcS_{2a}$)	2.1 (0.85)	10 (0.15)
MCF-7 cells (only QDs)	5.5 (0.58)	18 (0.42)
MCF-7 cells (QD-$AlPcS_{2a}$)	0.8 (0.93)	6.6 (0.07)

The considerable decrease in the QD lifetime is very significant since it confirms that FRET between the Tat-QDs and the phthalocyanine can occur in cells, with the major shorter lifetime component close to the value observed for QD-phthalocyanine complexes in aqueous solution.

The QDs and phthalocyanine must be in close proximity since the QD lifetime is quenched due to FRET. Since the QDs are efficiently taken up by cells owing to the Tat conjugation with the PEG layer, in contrast to QDs encapsulated with PEG only, it is proposed that endocytosis of intact QD-phthalocyanine complexes occurs. This would ensure that the QD and $AlPcS_{2a}$ remain associated, and Figure 2 demonstrates good co-localisation of the QD and $AlPcS_{2a}$. In support of this mechanism, Bonneau et al., demonstrated lysosomal localisation in fibroblasts following incubation with low density lipoprotein (LDL) – $AlPcS_{2a}$ complexes, which owing to their size would be taken up via endocytosis.[52] Although it is possible that some disulfonated phthalocyanine molecules partition to the cell membrane during endocytosis, they can then still co-localise with the QDs in endo/lysosomes after 24 h since the phthalocyanine can bind to the endo/lysosomal membranes, as is well documented for this molecule.[17,52] In this case, any membrane-bound phthalocyanine would be close to the Tat-QDs residing on the inner surface of the lysosomal membrane.[5] This close confinement could augment and stabilise phthalocyanine complexation with the quantum dots, since the phthalocyanine can then partition to the PEGylated layer of the QD.

3. Conclusion

We have shown that Tat-QD-phthalocyanine complexes can perform as efficient donor/acceptor pairs for FRET in cellular environments using confocal imaging and FLIM. Good correlation was observed between time-resolved emission lifetime measurements made in solution and cells which is remarkable given the complexity of the cellular environment. In particular, the substantial shortening in the QD lifetime demonstrates that efficient FRET occurs between QD-donor and phthalocyanine-acceptor in living cells. Excitation of the QD results in singlet oxygen generation via FRET to the phthalocyanine, and we demonstrated that this process could lead to photo-induced intracellular redistribution of Tat-conjugated QDs from their initial endo/lysosomal localisation. The localisation of the Tat-QDs on the inner surface of the endo/lysosomal membranes would favour reaction of singlet oxygen with membrane components. Although generation of reactive oxygen species from QDs has been reported in our study we found no evidence for photo-induced redistribution using the QDs alone at the visible wavelengths employed and the relatively low power irradiation regime.[22] This does not exclude the possibility that using more intense irradiation with UV excitation, where the QD absorption is very high, could induce a similar effect. In addition to the FRET mechanism, we also observed that direct excitation of the phthalocyanine to produce singlet oxygen can induce release

of the QDs from endo/lysosomes. These results are in accordance with the concept of photochemical internalisation (PCI) which has been developed for improving delivery of agents entrapped within endo/lysosomes, therefore PCI using a quantum dot incorporating both a photosensitiser and a bioactive agent should be feasible.[17,39] Release of QDs from the endo/lysosomal compartment using the PCI technique with visible light may find applications in studies of QDs and other nanoparticles taken up via endocytosis, since many studies have high-lighted the problems encountered with the persistence of endo/lysosomal trapping of QDs which remains a major challenge in QD delivery to selected intracellular sites.[59–61] This technique may therefore be of value to further investigations on cellular interactions of quantum dots.

4. Experimental Section

4.1. Materials

CdSe/ZnS quantum dots encapsulated with amine functionalised polyethylene glycol (PEG) and peak emission at 620 were purchased from Evident Technologies, Troy, US (EviTags™). The hydrodynamic diameter was ~25 nm, according to the specifications provided by Evident. Aluminium disulfonated phthalocyanine ($AlPcS_{2a}$) with two adjacent sulfonated groups was provided by Frontier Scientific, US. Rose Bengal, sodium azide (NaN_3), deuterium oxide (D_2O), Phosphate Buffered Saline (PBS), and DMEM: F12 medium were obtained from Sigma Aldrich, UK. Lysotracker Green was purchased from Life Technologies (Invitrogen) Ltd, UK.

4.2. Tat-peptide Conjugation to QDs

Amine functionalised QDs were conjugated with the HIV-1 Tat 48–57 sequence wherein the peptide was extended at the C-terminus by the tetrapeptide amide, GYKC-NH_2. The QDs were derivatised using Sulfo-SMCC (Sulfosuccinimidyl-4-[N-maleimidomethyl] cyclohexane-1-carboxylate) as a crosslinker (Sigma-Aldrich, UK) to introduce the thiol-reactive maleimido function required for conjugation with C-terminal cysteine of the peptide. Details of the peptide synthesis are provided elsewhere.[14] In brief, SulfoSMCC (0.6 mg) was dissolved in 1X PBS (200 Ml). The resulting solution was added to 200 μL of QD solution in an Eppendorf vial. The mixture was allowed to stand at room temperature for 1 hr. The reaction mixture was then concentrated to about 200 μL by microfiltration (6000 rpm, 8 min) and washed on the filter with PBS (2 × 200 μL). The solution was passed through a desalting column, previously equilibrated with deionised H_2O. The fraction containing the QDs was collected, ultrafiltered again to obtain a volume of 100 μL. The solution was transferred to an Eppendorf vial and 100 μL of conjugation buffer were added. To this solution, TAT-1 peptide (3 mg) were added, dissolved in 200 μL of conjugation buffer. The mixture was incubated at 4 °C overnight. The mixture was transferred to a microfilter and concentrated to 200 μL (6000 rpm, 10 min). The concentrate was washed twice on the filter with 500 μL of deionised water, and the volume was reduced to 200 μL.

4.3. Absorption and Emission Measurements

For the steady state photoluminescence measurements solutions were prepared of QD-$AlPcS_{2a}$ complexes at various ratios of PS/QDs (PS/QD: 0–8) in PBS and incubated in the dark for at least 15 min. The concentration of QDs was kept fixed (100 nM), while the concentration of PS was titrated from 100 to 800 nM. This direct preparation method using dilute solutions was employed since the limited water solubility of the $AlPcS_{2a}$ prohibited initial preparation of concentrated solutions, which would have resulted in strong aggregation of the $AlPcS_{2a}$. The solutions were placed in a 1 cm optical path quartz cuvette, and the emission spectra were recorded using a USB4000 Ocean Optics fibre-optic CCD spectrometer. Absorption spectra were measured using a Perkin-Elmer Lambda 25 UV/Vis spectrometer with quartz cuvette.

4.4. FRET Analysis

The overlap integral *J* which is the quantitative measure of donor/acceptor spectral overlap was calculated using the equation:

$$J = \int^{\infty} f_D(\lambda)\varepsilon_A(\lambda)\lambda^4 d\lambda$$

where $f_D(\lambda)$ is the fluorescence emission with $\int_0^{\infty} F(\lambda)d\lambda = 1\varepsilon(\lambda)$ is the exctinction coefficient and λ is the wavelength. The Förster distance, R_0, or the distance between the donor and acceptor at which the FRET efficiency is 50%, was calculated in nm using the equation

$$R_0 = 0.02108\ \left(k^2 \Phi n^{-4} J\right)^{1/6}$$

where $k^2 = 2/3$ (k is the orientation factor), Φ (the QD PL quantum yield) was set at 0.5, and *n* the refractive index. The overlap integral was calculated as 4.74×10^{15} M^{-1} cm^{-1} nm^4, and R_0 was then derived as 5.9 nm.[21,62]

The FRET efficiency for donor/acceptor pairs was measured using equation

$$E = 1 - (\tau_{DA} / \tau_D)$$

where the τ_{DA} and τ_D are the amplitude-weighted average fluorescence lifetime of the donor in the presence and absence of the acceptor, respectively.[21]

4.5. Lifetime Measurements

Photoluminescence lifetimes of QDs were measured; using time correlated single photon counting (TCSPC). Dilute solutions of QDs and QD complexes at various molar ratios were prepared and placed in a 1 cm optical path quartz cuvette. A pulsed laser diode module Edinburgh instrument Ltd., UK model EPL-405 was used to excite the samples at 405 nm at a 1 MHz repetition rate (EPL-405, Edinburgh Instruments Ltd., UK). The emission was detected using a fast multialkali photomultiplier module (model H5773–04, Hamamatusu Photonics K.K., Japan) via a longpass filter (OG510, Schott, UK) and a monochromator (model M300, Bentham Instrument Ltd, UK). A Lyot depolarizer (Thorlabs Ltd, Ely, UK) was incorporated to minimise any polarisation anisotropy artefacts. TCSPC was carried out using a PC-mounted TCSPC board (TimeHarp, Picoquant GmbH, Germany) and lifetimes were derived using Fluofit

NANO MICRO small

software (PicoQuant GmbH, Germany). A picosecond 635 nm laser module operating at 5MHz, 80 ps pulse duration (Picoquant GmbH, Germany), was used to excite to the phthalocyanine in the presence and absence of QDs to investigate the effect of QD binding on the phthalocyanine lifetime. The Instrument Response Function (IRF) was obtained from a non-fluorescent scattering Ludox solution (Sigmal-Aldrich, Gillingham, UK). Optimum fitting with minimisation of the residuals was confirmed using a Chi-squared value $\chi^2 < 1.4$.

4.6. Singlet Oxygen Measurements

The singlet oxygen phosphorescence at 1270 nm was detected using time-resolved photon counting from air-equilibrated, deuterated aqueous solutions in quartz cuvettes. For detection in the near-IR, a thermoelectrically cooled photomultiplier (model H10330–45, Hamamatsu Photonics Ltd, Hertfordshire, UK) was used, and emission was collected via a series of lenses from the cuvette in combination with a long-pass and a band-pass filter centred at 1270 nm (Infrared Engineering Ltd, Essex, UK). The solutions were excited using a 532 Nd:YAG laser (Lumanova GmbH, Germany) with the beam axis aligned orthogonally to the collection optics. The laser was pulsed at a repetition rate of 3 kHz and a pulse length of 3 ns, giving a mean power of 8 mW, and a fast photodiode (1 ns rise time, Becker-Hickl, Berlin, Germany) was used to synchronise the laser pulse with the photon counting detection system. A series of neutral density filters was used to attenuate the laser power. The photon counting equipment consisted of a PC-mounted multiscaler board (model MSA-300, Becker-Hickl, Berlin, Germany) and a pre-amplifier (Becker-Hickl, Berlin, Germany) which gave a resolution of 5 ns per channel. Time-resolved phosphorescence measurements were accumulated by the multiscaler board. The traces were analysed using FluoFit software (PicoQuant GmbH, Berlin, Germany) to extract the singlet oxygen decay lifetime. To calculate the quantum yield, Rose Bengal was used as the standard with a quantum yield of 0.76 in D_2O with the concentration adjusted to give the same absorbance as the QD solution.[63,64] To analyse the results we used the time-gated integration method instead of the more commonly used zero-intercept method.[46,65] The latter was prohibited by the relatively high but short-lived photoluminescence residual signal from the QDs at lower phthalocyanine/QD molar ratios. Integration of the signal from 25–50 μs avoided this interference since the photoluminescence had completely decayed before this time range.

4.7. Cell Culture and Confocal Imaging

Human breast carcinoma cells (MCF-7, European Collection of Animal Cell cultures, UK) were cultivated in Dulbecco's Modified Eagle's Medium (DMEM-F12) supplemented with 10% foetal calf serum (FCS, Sigma-Aldrich, UK) and Gentamicin Gibco BRL, Life Technologies Ltd, Paisley, UK at 37 °C in a humidified atmosphere containing 5% CO_2. For imaging, cells were cultured onto glass-bottomed Petri dishes (FluoroDish, World Precision Instruments Ltd., UK). The following day, the medium was discarded and replaced with fresh FCS free media (to prevent competitive binding of the phthalocyanine to serum proteins) containing QDs or QD-$AlPcS_{2a}$. After overnight incubation, cells were rinsed three times with PBS and were replaced with 10% FCS in phenol red free medium. For the intracellular distribution study of Tat-conjugated QDs, cells were incubated with FCS free medium containing QDs (25 nM) for 24 h. After 24 h, the medium was removed and cells were incubated with LysoTracker Green (100 nM) in growth medium for 30 min at 37 °C. Afterwards, the cells were rinsed three times with PBS and fresh FCS; phenol red free media was added to each dish. Images were acquired with a LSCM (FV-1000, Olympus, Japan), 60x water emersion objective. The multichannel function was used to collect three sets of images: (a) using QD donor excitation at 488 nm, donor emission (590–640 nm) and phthalocyanine acceptor emission (670–700 nm) channels for QD and FRET imaging; (b) 633 nm excitation and emission (670–700 nm) channel for phthalocyanine imaging; (c) 488 nm excitation and emission channel (500–530 nm) for imaging LysoTracker Green fluorescence. Confocal images were acquired using proprietary software (Olympus Fluoview) and then displayed and analysed using Image J (NIH, US).

4.8. Fluorescence Lifetime Imaging Microscopy

Cells were prepared as described above and imaged using an inverted microscope (Leica TCS SP2) equipped with a FLIM system (Becker and Hickl, SPC830, TCSPC) at the Dept. of Physics, King's College London. Samples were excited with a pulsed picosecond diode laser emitting at 470 nm at 1 MHz repetition rate (Hamamatsu Photonics KK, Japan, model PLP-10, 90 ps pulse duration). Photoluminescence of QDs and phthalocyanine fluorescence were collected in the donor and acceptor channels, respectively via bandpass filters centred at 620 ± 15 nm for the QD and 690 ± 20 nm for the phthalocyanine (620DF30 and 690DF40, Omega Optical Inc. US) respectively. Images were analysed using SPC Image software (Becker & Hickl GmbH, Germany).

Supporting Information

Supporting Information is available from the Wiley Online Library or from the author. Supporting Information Available: (1) Molecular structure of $AlPcS_{2a}$ and steady-state photoluminescence emission spectra of pure QDs and QD-$AlPcS_{2a}$ complexes, (2) Spectral overlap between QD-$AlPcS_{2a}$ complexes (3) Confocal imaging showing co-localisation of Tat-conjugated CdSe/ZnS QDs and LysoTracker Green in MCF-7 cells (4) Lifetime decays of Tat-conjugated CdSe/ZnS QDs in the absence and presence of $AlPcS_{2a}$ in MCF-7 cells.

Acknowledgements

We are grateful for the use of the confocal microscopy facilities at the London Centre for Nanotechnology. We acknowledge support for Elnaz Yaghini (BB/J009318/1) and Francesca Giuntini (BB/D0127831) from the Biotechnology and Biological Sciences Research Council.

[1] U. Resch-Genger, M. Grabolle, S. Cavaliere-Jaricot, R. Nitschke, T. Nann, *Nat. Methods* **2008**, *5*, 763.
[2] W. Jiang, E. Papa, H. Fischer, S. Mardyani, W. C. Chan, *Trends Biotechnol.* **2004**, *22*, 607.
[3] J. M. Klostranec, W. C. W. Chan, *Adv. Mater.* **2006**, *18*, 1953.
[4] M. Green, *Angew. Chem. Int. Ed.* **2004**, *43*, 4129.
[5] G. Ruan, A. Agrawal, A. I. Marcus, S. Nie, *J. Am. Chem. Soc.* **2007**, *129*, 14759.
[6] S. R. Schwarze, A. Ho, A. Vocero-Akbani, S. F. Dowdy, *Science* **1999**, *285*, 1569.
[7] G. Drin, S. Cottin, E. Blanc, A. R. Rees, J. Temsamani, *J. Biol. Chem.* **2003**, *278*, 31192.
[8] A. Eguchi, T. Akuta, H. Okuyama, T. Senda, H. Yokoi, H. Inokuchi, S. Fujita, T. Hayakawa, K. Takeda, M. Hasegawa, M. Nakanishi, *J. Biol. Chem.* **2001**, *276*, 26204.
[9] A. Ferrari, V. Pellegrini, C. Arcangeli, A. Fittipaldi, M. Giacca, F. Beltram, *Mol .Ther.* **2003**, *8*, 284.
[10] S. Santra, H. Yang, J. T. Stanley, P. H. Holloway, B. M. Moudgil, G. Walter, R. A. Mericle, *J. Am. Chem. Soc.* **2005**, *127*, 3144.
[11] F. L. Xue, J. Y. Chen, J. Guo, C. C. Wang, W. L. Yang, P. N. Wang, D. R. Lu, *J. Fluoresc.* **2007**, *17*, 149.
[12] J. T. Wang, K. Berg, A. Hogset, S. G. Bown, A. J. MacRobert, *Photochem. Photobiol. Sci.* **2013**, *12*, 519.
[13] K. Berg, S. Nordstrand, P. K. Selbo, D. T. Tran, E. Angell-Petersen, A. Hogset, *Photochem. Photobiol. Sci.* **2011**, *10*, 1637.
[14] J. T. Wang, F. Giuntini, I. M. Eggleston, S. G. Bown, A. J. MacRobert, *J. Controlled Release* **2012**, *157*, 305.
[15] A. Weyergang, P. K. Selbo, K. Berg, *J. Controlled Release* **2006**, *111*, 165.
[16] J. Woodhams, P. J. Lou, P. K. Selbo, A. Mosse, D. Oukrif, A. MacRobert, M. Novelli, Q. Peng, K. Berg, S. G. Bown, *J. Controlled Release* **2010**, *142*, 347.
[17] P. K. Selbo, A. Weyergang, A. Hogset, O. J. Norum, M. B. Berstad, M. Vikdal, K. Berg, *J. Controlled Release* **2010**, *148*, 2.
[18] H. L. Lu, W. J. Syu, N. Nishiyama, K. Kataoka, P. S. Lai, *J. Controlled Release* **2011**, *155*, 458.
[19] W. R. Algar, U. J. Krull, *Anal. Bioanal. Chem.* **2008**, *391*, 1609.
[20] A. R. Clapp, I. L. Medintz, H. Mattoussi, *ChemPhysChem* **2006**, *7*, 47.
[21] J. R. Lakowicz, *Principles of Fluorescence Spectroscopy*, Springer, New York, **2006**.
[22] E. Yaghini, A. M. Seifalian, A. J. MacRobert, *Nanomedicine* **2009**, *4*, 353.
[23] A. C. S. Samia, X. B. Chen, C. Burda, *J. Am. Chem. Soc.* **2003**, *125*, 15736.
[24] J. M. Tsay, M. Trzoss, L. X. Shi, X. X. Kong, M. Selke, M. E. Jung, S. Weiss, *J. Am. Chem. Soc.* **2007**, *129*, 6865.
[25] C. Y. Hsu, C. W. Chen, H. P. Yu, Y. F. Lin, P. S. Lai, *Biomaterials* **2013**, *34*, 1204.
[26] O. J. Norum, J. V. Gaustad, E. Angell-Petersen, E. K. Rofstad, Q. Peng, K. E. Giercksky, K. Berg, *Photochem. Photobiol.* **2009**, *85*, 740.
[27] N. Maman, S. Dhami, D. Phillips, D. Brault, *Biochim. Biophys. Acta* **1999**, *1420*, 168.
[28] D. Phillips, S. Dhami, R. Ostler, Z. Petrasek, *Prog. React. Kinet. Mech.* **2003**, *28*, 299.
[29] A. M. Dennis, G. Bao, *Nano. Lett.* **2008**, *8*, 1439.
[30] A. R. Clapp, I. L. Medintz, J. M. Mauro, B. R. Fisher, M. G. Bawendi, H. Mattoussi, *J. Am. Chem. Soc.* **2004**, *126*, 301.
[31] H. E. Grecco, K. A. Lidke, R. Heintzmann, D. S. Lidke, C. Spagnuolo, O. E. Martinez, E. A. Jares-Erijman, T. M. Jovin, *Microsc. Res. Technol.* **2004**, *65*, 169.
[32] A. Sillen, Y. Engelborghs, *Photochem. Photobiol.* **2008**, *68*, 475.
[33] O. J. Rolinski, D. J. S. Birch, *J. Chem. Phys.* **2000**, *112*, 8923.
[34] E. A. Jares-Erijman, T. M. Jovin, *Nat. Biotechnol.* **2003**, *21*, 1387.
[35] M. Ambroz, A. Beeby, A. J. MacRobert, M. S. Simpson, R. K. Svensen, D. Phillips, *J. Photochem. Photobiol. B* **1991**, *9*, 87.
[36] M. Ambroz, A. J. MacRobert, J. Morgan, G. Rumbles, M. S. Foley, D. Phillips, *J. Photochem. Photobiol. B* **1994**, *22*, 105.
[37] L. X. Shi, B. Hernandez, M. Selke, *J. Am.Chem. Soc.* **2006**, *128*, 6278.
[38] J. Ma, J. Y. Chen, M. Idowu, T. Nyokong, *J. Phys. Chem. B* **2008**, *112*, 4465.
[39] A. Hogset, L. Prasmickaite, P. K. Selbo, M. Hellum, B. O. Engesaeter, A. Bonsted, K. Berg, *Adv. Drug Delivery Rev.* **2004**, *56*, 95.
[40] Y. Cheng, A. C. Samia, J. Li, M. E. Kenney, A. Resnick, C. Burda, *Langmuir* **2010**, *26*, 2248.
[41] Y. Cheng, J. D. Meyers, A. M. Broome, M. E. Kenney, J. P. Basilion, C. Burda, *J. Am. Chem. Soc.* **2011**, *133*, 2583.
[42] B. Jang, J. Y. Park, C. H. Tung, I. H. Kim, Y. Choi, *ACS Nano* **2011**, *5*, 1086.
[43] C. Wang, H. Tao, L. Cheng, Z. Liu, *Biomaterials* **2011**, *32*, 6145.
[44] H. Mojzisova, S. Bonneau, P. Maillard, K. Berg, D. Brault, *Photochem. Photobiol. Sci.* **2009**, *8*, 778.
[45] C. Cantau, T. Pigot, N. Manoi, E. Oliveros, S. Lacombe, *ChemPhysChem* **2007**, *8*, 2344.
[46] S. M. Bishop, A. Beeby, H. Meunier, A. W. Parker, M. S. C. Foley, D. Phillips, *J. Chem. Soc. Faraday Trans.* **1996**, *92*, 2689.
[47] M. K. Kuimova, G. Yahioglu, P. R. Ogilby, *J. Am. Chem. Soc.* **2009**, *131*, 332.
[48] A. C. S. Samia, X. B. Chen, C. Burda, *J. Am. Chem. Soc* **2003**, *125*, 15736.
[49] K. Suhling, P. M. W. French, D. Phillips, *Photochem. Photobiol. Sci.* **2005**, *4*, 13.
[50] W. Becker, *J. Microsc.* **2012**, *247*, 119.
[51] J. W. Borst, A. J. W. G. Visser, *Meas. Sci. Technol.* **2010**, *21*.
[52] S. Bonneau, P. Morliere, D. Brault, *Biochem. Pharmacol.* **2004**, *68*, 1443.
[53] R. M. Clegg, O. Holub, C. Gohlke, *Biophotonics* **2003**, *360*, 509.
[54] F. G. Haj, P. J. Verveer, A. Squire, B. G. Neel, P. I. H. Bastiaens, *Science* **2002**, *295*, 1708.
[55] T. Ng, A. Squire, G. Hansra, F. Bornancin, C. Prevostel, A. Hanby, W. Harris, D. Barnes, S. Schmidt, H. Mellor, P. I. H. Bastiaens, P. J. Parker, *Science* **1999**, *283*, 2085.
[56] M. Peter, S. Ameer-Beg, *Biol. Cell* **2004**, *96*, 231.
[57] P. R. Selvin, *Nat. Struct. Biol.* **2000**, *7*, 730.
[58] F. Festy, S. M. Ameer-Beg, T. Ng, K. Suhling, *Mol. Biosyst.* **2007**, *3*, 381.
[59] J. B. Delehanty, C. E. Bradburne, K. Boeneman, K. Susumu, D. Farrell, B. C. Mei, J. B. Blanco-Canosa, G. Dawson, P. E. Dawson, H. Mattoussi, I. L. Medintz, *Integr. Biol.* **2010**, *2*, 265.
[60] V. Sigot, D. J. Arndt-Jovin, T. M. Jovin, *Bioconjug. Chem.* **2010**, *21*, 1465.
[61] H. W. Duan, S. M. Nie, *J. Am. Chem. Soc.* **2007**, *129*, 3333.
[62] S. E. Braslavsky, E. Fron, H. B. Rodriguez, E. S. Roman, G. D. Scholes, G. Schweitzer, B. Valeur, J. Wirz, *Photochem. Photobiol. Sci.* **2008**, *7*, 1444.
[63] C. Tanielian, C. Wolff, M. Esch, *J. Phys. Chem.* **1996**, *100*, 6555.
[64] R. W. Redmond, J. N. Gamlin, *Photochem. Photobiol.* **1999**, *70*, 391.
[65] C. Cantau, T. Pigot, N. Manoi, E. Oliveros, S. Lacombe, *ChemPhysChem* **2007**, *8*, 2344.

Received: May 10, 2013
Revised: July 2, 2013
Published online: September 13, 2013

